Journal of the Chilean Chemical Society

A COMPLEMENTARY VIEW TO THE BONDING PATTERN IN THE N_5^+ CATION: AN ELECTRON LOCALIZATION FUNCTION AND LOCAL TEMPERATURE ANALYSIS

E. Chamorro*

Departamento de Ciencias Químicas, Facultad de Ecología y Recursos Naturales, Universidad Andrés Bello, República 217, Santiago, Chile. E-mail:echamorro@abello.unab.cl
(Received: August 6, 2003 - Accepted : August 18, 2003)

The electron localization function (ELF), a local measure of the Pauli repulsion effect, and the local Kohn-Sham temperature analysis, which is defined within the framework of a local thermodynamics description of density functional theory, have been used to explore the bonding characteristics in the open chain N_5^+ cation. It is found that both the ELF and local temperature maps depict uniquely the regions of pair localizations, yielding a description of bonding which agrees and complements previous techniques of analysis. Particularly, the three-center four-electron interaction in the NNN terminal atoms of N_5^+ and the contribution of terminal triple bonds to the bonding nature of the cation have been characterized in detail from the electron fluctuation among ELF basins populations. The features of bonding in terms of the local kinetic energy analysis have been visualized directly from the analysis of local temperature map.

I. INTRODUCTION

Recently, it has been shown by Ponec[1] that the nontrivial bonding pattern at the N_5^+ cation can be rationalized in terms of the following resonance schemes,

(la)

(lb)
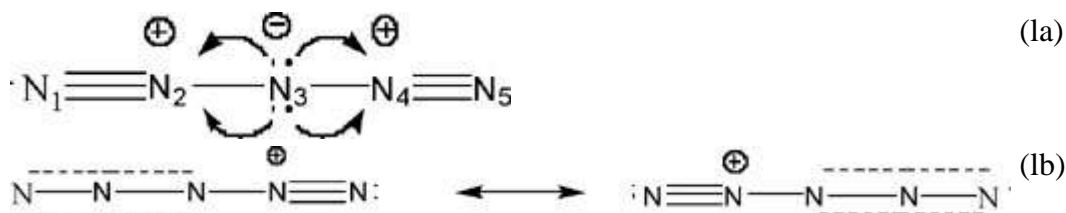
These structures emphasize the contribution of terminal triple bonds to the bonding pattern and, also, that lone electron pairs on the central nitrogen are being effectively delocalized towards neighboring atoms. This non-classical NNN interaction depicted in Eq. (1b) has been characterized in terms of a three-center four-electron (3c-4e) type of bonding similar to the one observed in the precursor azide ion.[1] Results derived from the nonlinear population analysis schemes[2] and also from the domain (Ω) averaged Fermi hole analysis,[3] are in agreement with the Valence Bond (VB) methodology of Harcourt and Klapotke,[4] and with the previous proposals of Nguyen

and Ha concerning structures like 1b.[5] It is clear however from these studies that a complete visualization (i.e., fluctuation of electron density and delocalization) of this type of bond interaction has not been completely achieved.

In the context of research for the *rationalization* and *characterization* of bonding in this intriguing cationic molecular structure, it would be interesting to further examine the problem of bonding pattern within the framework of a local characterization of the molecular space. In this sense, the topological analysis of the electron localization function (ELF)[6] constitutes a simple and elegant tool which has been shown of complementary value in several problems of chemical reactivity.[7] In addition, we have also explored the usefulness of the Kohn-Sham local temperature index[8] in the context of pair localization, a chemical reactivity issue which has been reviewed recently by Ayers, Parr and Nagy.[9] Our aim is to further examine the N_5^+ bonding pattern, particularly the details of "triple" and "single" bonding interactions along the open chain of N_5^+ structure as suggested by Eq. (1), and to compare it with previously used methodologies of analysis. It will be shown that a simple and complementary characterization of bonding is clear from the ELF and local temperature topological maps.

The electron localization function (ELF) scheme

Topological analysis (i.e. gradient field analysis) of well-defined local functions provides an elegant approximation to a rigorous quantitative and qualitative analysis. Both the atoms-in-molecules (AIM) theory and the topological analysis of the electron localization function (ELF) of Becke and Edgecombe,[11] provide us with a useful partition of the molecular space into basins of attractors related with intuitive concepts of chemical bonding. Open subsystems (i.e. basins) associated with "atoms" regions arise in the AIM theory while "pair regions" does it in the ELF scheme.[7] Comprehensive reviews concerning the details of this technique of topological analysis have been published elsewhere.[7,12] It must be also pointed out here that the domain-averaged analysis previously presented by Ponec,[1] was carried out in the framework of atomic regions. It is clear that ELF will be a complementary and direct choose to deal with bonding and nonbonding *pair* regions in molecules.

The local function ELF(r) can be interpreted in terms of the excess of local kinetic energy density due to the Pauli repulsion, $T(\rho(r))$, and the Thomas-Fermi kinetic energy density, $T_h(\rho(r))$,[7,13]

$$ELF(\mathbf{r}) = \left[1 + \left[\frac{T(\mathbf{r})}{T_h(\mathbf{r})} \right]^2 \right]^{-1} \tag{2}$$

The scaled function ELF (i.e., valued from 0 to 1) was first introduced by Becke and Edgecombe in the framework of a Taylor expansion characterization of the pair density function $P(r,s) = \frac{1}{2} s^2 T(r) + ...$[7] Henceforth, highest values of ELF ($\rightarrow 1$) are obtained within a pair region, and lower value one ($\rightarrow 0$) are associated to the border separation between two such pair regions. The homogeneous electron gas (i.e., Thomas-Fermi) is taken as a reference for simple normalization, being the ELF value of $\frac{1}{2}$ in this case. For an arbitrary single determinantal (i.e. a single Slater determinant) wave function,

built from Hartree-Fock (HF) or Kohn-Sham (KS) orbitals, $\varphi_i(r)$, it can be straightforward written that

$$T(\mathbf{r}) = \frac{1}{2}\sum_i |\nabla\varphi_i(\mathbf{r})|^2 - \frac{1}{8}\frac{|\nabla\rho(\mathbf{r})|^2}{\rho(\mathbf{r})}, \qquad (3)$$

$$T_h(\mathbf{r}) = 2.871\rho(\mathbf{r})^{5/3}, \qquad (4)$$

$$\rho(\mathbf{r}) = \sum_i |\varphi_i(\mathbf{r})|^2, \qquad (5)$$

where atomic units are implicit in all equations. The integration of density r(r) over the basins of attractors associated with the gradient field of ELF, yields properties that can be consistently interpreted in connection with relevant chemical bonding characteristics. The intuitive concepts of localization and delocalization of the electron density[1] are recovered through a standard topological population analysis.[7b, c] The average population of a basin, $\tilde{N}_i$, obtained from the integral of the one electron density over the volume of the basin,

$$\tilde{N}_i = \int_{\Omega_i} \rho(\mathbf{r})d\mathbf{r}, \qquad (6)$$

[1]R. F. W. Bader, Localization and delocalization in quantum chemistry, Edited by O. Chalvet, et. al. (Reidel, Dordrecht, 1976), Vol 1.

and their population variance, $\sigma^2(\tilde{N}_i)$ (i.e., the quantum uncertainty of the basin population), can therefore be calculated in terms of the diagonal elements of the first $\rho(r)$ and second order $\pi(r_1,r_2)$ density matrices,

$$\sigma^2(\tilde{N}_i) = \int_{\Omega_i} d\mathbf{r}_1 \int_{\Omega_i} d\mathbf{r}_2 \pi(\mathbf{r}_1,\mathbf{r}_2) + \tilde{N}_i - [\tilde{N}_i]^2. \qquad (7)$$

Furthermore, it has been shown that the variance of a given basin population can be written explicitly in terms of a sum of contributions arising from the other basins,

$$\sigma^2(\tilde{N}_i) = \sum_{j\neq i} \tilde{N}_i\tilde{N}_j - B_{ij}, \qquad (8)$$

$$B_{ij} = \int_{\Omega_i} d\mathbf{r}_1 \int_{\Omega_j} d\mathbf{r}_2 \rho(\mathbf{r}_1)\rho(\mathbf{r}_2) + \int_{\Omega_i} d\mathbf{r}_1 \int_{\Omega_j} d\mathbf{r}_2 \rho_{XC}(\mathbf{r}_1,\mathbf{r}_2),$$

where $\rho_{XC}(r_1, r_2)$ stands for the exchange-correlation density.[7] Henceforth, the covariance (i.e. inter basin) analysis constitutes itself a useful tool for a detailed examination of the electronic delocalization in the molecular framework.[15] Indeed, the Bader relative fluctuation index $\lambda(\tilde{N}_i)$, is an efficient tool to study delocalization,

$$\lambda(\tilde{N}_i) \doteq \frac{\sigma^2(\tilde{N}_i)}{\tilde{N}_i}.$$

(9)

The local temperature descriptor, $\Theta(r)$, in the context of pair electron localization

A local thermodynamics description of electrons in atoms and molecules has been introduced in the framework of the ground state density functional theory.[9] Within such a description, the Kohn-Sham inhomogeneous "ideal gas", understood like a reference system, with the same electron density $\rho(r)$ of the real one, has associated a local quantum temperature $\Theta(r)$. This quantity is defined, by *analogy* with classical statistical thermodynamics, in terms of corresponding local kinetic energy density, (i.e., of the Kohn-Sham reference system), $t_{KS}(r)$,

$$t_{KS}(\mathbf{r}) \equiv \frac{3}{2} k_B \rho(\mathbf{r}) \Theta(\mathbf{r}).$$

(10)

The local temperature is essentially a measure of the kinetic energy of electrons in the quantum fluid electron cloud, and the fundamental equation of density functional theory can be therefore written as,

$$\mu = \frac{3}{2} k_B \Theta(\mathbf{r}) + \frac{3}{2} k_B \int \rho(\mathbf{r}) \Theta(\mathbf{r}, \mathbf{r_1}) d\mathbf{r_1} + v_{xc}(\mathbf{r}) + v_H(\mathbf{r}) + v(\mathbf{r}),$$

(11)

where m is the chemical potential, k_B is the Boltzman constant, $v_{xc}(r)$ is the exchange correlation potential, $v_H(r)$ is the Hartree potential, $v(r)$ is the external potential (i.e. due to the a nuclei of charge Z_a and position R_α and other fields), and $\Theta(r, r_1)$ is a response function associated with the local temperature,

$$\mathbf{v}_{xc}(\mathbf{r}) \equiv \frac{\delta E_{xc}[\rho(\mathbf{r})]}{\delta \rho(\mathbf{r})}$$

$$\mathbf{v}_{H}(\mathbf{r}) \equiv \int \frac{\rho(\mathbf{r}_1)}{|\mathbf{r}-\mathbf{r}_1|} d\mathbf{r}_1$$

$$v(\mathbf{r}) \equiv \sum_{\alpha} \frac{Z_{\alpha}}{|\mathbf{r}-\mathbf{R}_{\alpha}|} + .. \qquad (12)$$

$$\Theta(\mathbf{r},\mathbf{r}_1) \equiv \frac{\delta\Theta(\mathbf{r})}{\delta\rho(\mathbf{r}_1)}$$

It must be explicitly pointed out that the kinetic energy density is not well defined[10] and therefore, Eq. (11) is arbitratry. The local temperature can be straightforward related to the Politzer average local ionization potential $I(r)$,[10]

$$\frac{3}{2}k_B\Theta(\mathbf{r}) + v_{KS}(\mathbf{r}) - \frac{1}{4}\nabla^2\rho(\mathbf{r}) = I(\mathbf{r}) \equiv \frac{\sum_{i=1}^{N} -\varepsilon_i \rho_i(\mathbf{r})}{\rho(\mathbf{r})}, \qquad (13)$$

and therefore it is in close connection with the ideas of local chemical reactivity of the molecular system again electrophilic attacks. Of course, these molecular regions are evidently related with the regions where electrons are *more localized*. In this context, it has been also emphasized that, the local temperature constitutes a measure of the probability of observing two electrons in a region of space, and that it reflects a local measure of the Pauli principle.[10,16] By taking some reference to analyze regions of localization, the quantity $\nu(\mathbf{r})$ can be defined,[10]

$$\nu(\mathbf{r}) \equiv \frac{\Theta'(\mathbf{r})}{1+\Theta'(\mathbf{r})}, \qquad \Theta'(\mathbf{r}) \equiv \frac{\Theta_{ref}(\mathbf{r})}{\Theta_{ks}(\mathbf{r})}. \qquad (14)$$

which constitutes a descriptor that maps the topological characteristics of $\Theta(\mathbf{r})$ in Eq. (10) onto the range 0 to 1. It has been emphasized that $\nu(\mathbf{r})$ constitutes the localization orbital locator (LOL) index of Schmider and Becke[1] when the uniform gas is the reference system. Henceforth, regions with the highest probability to find localized pairs (i.e. regions with cooler local temperatures, or slower electrons, than the reference) are associated with values of $\nu(\mathbf{r}) > \frac{1}{2}$, and those ones with lower probability for localization of pairs of electrons (i.e. with higher local temperatures, or faster electrons, than the reference) are associated with $\nu(\mathbf{r}) < \frac{1}{2}$. Therefore, the

separation region for which $\nu(r) = ½$ will be important in order to identify and characterize several type of "bonds" in molecules and transition states.[17,18]

II. COMPUTATIONAL DETAILS

Ab-initio B3LYP/6-311G(d) optimized N_5^+ geometrical parameters have been obtained from Ref. [1] This level of theory is enough suitable for the goals of the present study. The corresponding wave function was obtained using the Gaussian 98 package of programs.[19] The topological analysis of the ELF and its associated population analysis have been performed using the TopMod suite of programs.[20,21] A simple modification has been introduced into the rho_int.f module in order to calculate the local temperatures indexes in Eq. (10) and Eq. (14). Graphical analysis has been done using the Vis5d[22] visualization tools.

III. RESULTS AND DISCUSSION

Table 1 reports the basin populations $\tilde{N}_i$, standard deviation $\sigma^2(\tilde{N}_i)$, relative fluctuation $\lambda(\tilde{N}_i)$, and main contributions of different basins i(%) to $\sigma^2(\tilde{N}_i)$ from the density obtained at the B3LYP/6-311G(d,p) level of theory. The observed gradient field yields directly to integrated populations over the localization regions which nicely agree with the picture of bonding represented by Eq. 1a. In effect, lone pairs regions at N1 and N5 are associated to the lone valence monosynaptic basins localizing 3.26e-each, while two monosynaptic valence basins are associated with the central nitrogen localizing 1.83 e-ach. Note that there is not monosynaptic valence basins associated with the N2 and N4 centers at this level of theory. It is also clear that lone pair populations at N3 are more delocalized ($\lambda=0.53$) than those associated the lone terminal pair region ($\lambda=0.36$). The valence disynaptic regions associated with the "triple" bonding interaction N1N2 and N5N4 are localizing 4.80e- each, while the "single" bonds N2N3 and N3N4 are localizing 1.83e each. Thus, the simple Lewis structure which arise from the ELF integrated basins yields directly to Eq. (1a). Note however, that at the same time, delocalization indexes shows that these "single" bond populations are the strongest delocalized in the system ($\lambda=0.57$). The relevance of this type of structure has been already emphasized by Ponec[1] in the framework of the Fermi hole analysis at atomic regions. The fluctuation analysis based in Eq. (7) and Eq. (8), yields directly to a complementary view of the simplified picture of bonding drawn in Eq. (1b). It can be noted, for instance, that the lone pair populations at N3 are being delocalized over the "single" N2N3 and N3N4 and the "triple" N1N2 and N4N5 bond regions up to 17.1%, and 8.1%, respectively. Indeed the "triple" bonding population contributes up to 68.4% to the corresponding lone pair at the terminal nitrogen center. From the fluctuation analysis in Table 1 we observe explicitly that the 3c-4e interaction is localized at the terminal centers. Figure 1 depicts the contour map for the localization domains of the electron localization function (ELF) corresponding to the N1N2N3 bond fragment of the N_5^+ cation. The detailed features of this interaction is, as will be shown below, more clear from a local temperature map representation.

Table 1. Basin populations $\tilde{N}_i$, standard deviation $\sigma^2(\tilde{N}_i)$, relative fluctuation $\lambda(\tilde{N}_i)$, and main contributions of other basins i(%) to $\sigma^2(\tilde{N}_i)$ for the N_5^+ cation from the density obtained at the B3LYP/6-311G(d,p) level of theory.

Basin	$\tilde{N}_i$	$\sigma^2(\tilde{N}_i)$	$\lambda(\tilde{N}_i)$	Contribution analysis (%)

1	C(N1)	2.10	0.28	0.14	6(50.9) 7(41.9)
2	C(N2)	2.10	0.30	0.14	6(10.4) 7(60.3) 8(22.0)
3	C(N3)	2.10	0.29	0.14	8(14.4) 9(29.3) 10(29.3) 11(14.4)
4	C(N4)	2.11	0.30	0.14	11(22.0) 12(60.3) 13(10.4)
5	C(N5)	2.10	0.28	0.14	12(41.9) 13(50.9)
6	V(N1)	3.26	1.17	0.36	1(12.4) 7(68.4)
7	V(N1,N2)	4.80	1.73	0.36	1(6.9) 2(10.5) 6(46.2) 8(23.5)
8	V(N2,N3)	1.85	1.06	0.57	2(6.3) 6(5.3) 7(38.5) 9(17.1) 10(17.1) 11(7.1)
9	V(N3)	1.83	0.97	0.53	3(8.7) 7(8.1) 8(18.6) 10(27.1) 11(18.6) 12(8.1)
10	V(N3)	1.83	0.97	0.53	3(8.7) 7(8.1) 8(18.6) 9(27.1) 11(18.6) 12(8.1)
11	V(N3,N4)	1.85	1.06	0.57	4(6.3) 8(7.1) 9(17.1) 10(17.1)12(38.5) 13(5.3)
12	V(N4,N5)	4.80	1.73	0.36	4(10.5) 5(6.9) 11(23.5) 13(46.1)
13	V(N5)	3.26	1.17	0.36	5(12.4) 12(68.4)

(A)   **(B)**
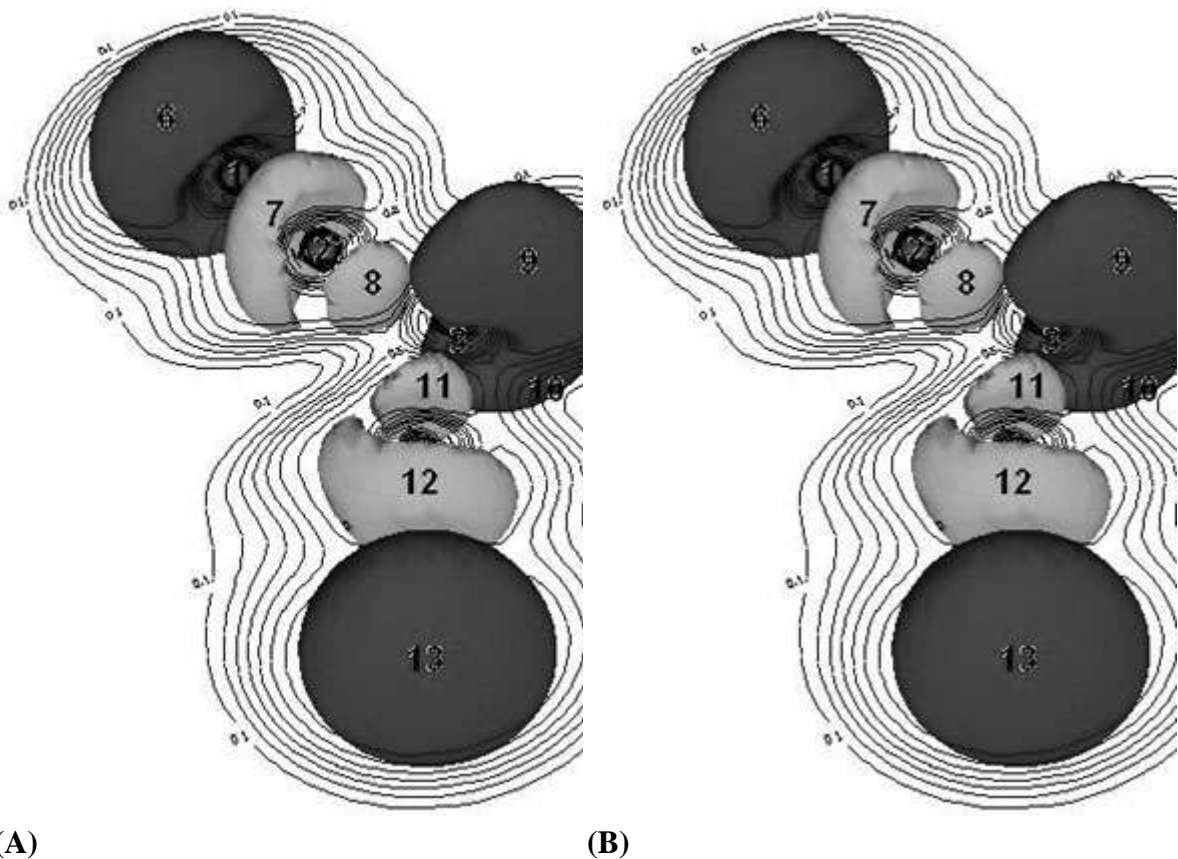
Fig. 1. (a) Localization domains of the electron localization function ELF at the N_5^+ specie. The ELF=0.80 isosurfaces were calculated from the optimized wave functions at the B3LYP-6-311G(d,p) level of theory. (b) Contour map of the ELF in the plane containing the N3N4N5 centers (equivalent to N1N2N3 by symmetry), and which is perpendicular to the molecular plane. Regions of higher probability to find electron pairs (i.e., regions with ELF(**r**) →□1), are indicated in red color. The ELF(**r**) → 0 regions are represented in blue, and the ELF → ½ regions (i.e., the Thomas Fermi gas reference) are represented by green tones.

With the aim to characterize in detail the delocalization pattern of the electron pairs along the N_5^+ cation, the corresponding bifurcation diagram is depicted in Figure 2. We can note immediately that the separation of the valence regions are in a small range of

ELF values between 0.74 and 0.77. The highest correlation which exists between the N1N2 and N2N3 centers is also clear. That is, the N2N3 population contributes to the N1N2 one up to a 23.5%, and the opposite trends rises up to 38.5%. The four disynaptic valence basins separates at the highest value of ELF=0.77, consistently with the higher inter-basin fluctuations associated with these regions.
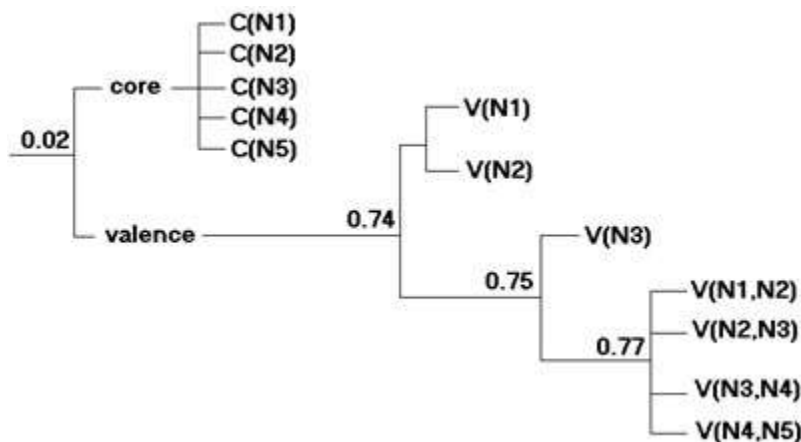
Fig. 2. Bifurcation diagram corresponding to the electron localization function (ELF) analysis at the N_5^+ cation from the optimized wavefunction at the B3LYP/6-311G(d,p) level of theory.

In Figure 3, the contour map for the variable $\nu(\mathbf{r})$, in Eq. (14), corresponding to the N_5^+ cation is depicted. Note the close agreement with the ELF picture in Figure 1. The $\nu=1/2$ contour is indicated with a black color line, separating "cold" and "hot" regions of bonding. That is, the "pairing" and "delocalized" regions, respectively, with respect to the Thomas-Fermi uniform electron gas. From this map, the bonding interaction[17,18] which exists between the "triple" N5N4 and "single" N4N3 bonds becomes more clear and explicitly manifest. The spatial distribution of this fluctuation is clearly depicted, in agreement with and resembling the ELF fluctuation results. The local temperature map emphasizes (i.e. from the n = 0.5 contour) the absence of formal *covalent*interactions between the N4N3 and the N5N4 pairs of nitrogen atoms. It is remarkable that the present simple analysis of ELF and temperature maps yields to a very comprehensive scheme for the understanding of chemical bonding in the structure of the N_5^+ cation.

(A)   **(B)**
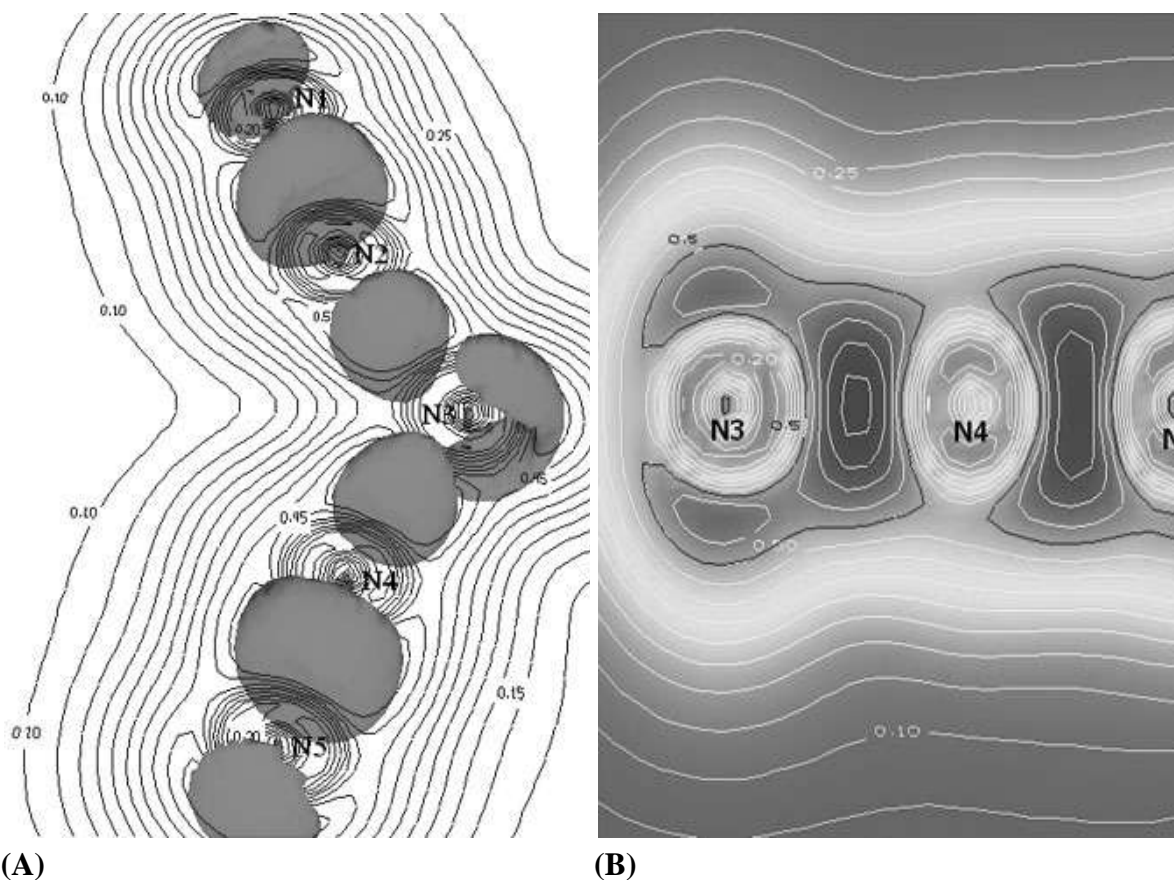
Fig. 3. (**a**) Isosurface map for the variable $\nu(\mathbf{r})$ for the value 0.57 corresponding to the N_5^+ cation from the optimized wave function at the B3LYP/6-311G(d,p) level of theory. (**b**) Contour map of the $n(\mathbf{r})$ variable in the plane containing the N3N4N5 centers (equivalent to N1N2N3 by symmetry), and which is perpendicular to the molecular plane. Regions in blue stands for "cooler" regions that the Thomas-Fermi reference uniform gas and henceforth they are associated with pair regions. "Hotter" regions have been indicated in red color and the temperature of the reference has been drawn in green tones. The regions enclosed by the line $\nu = \frac{1}{2}$ are associated with the regions of electron pairs (i.e., electrons are slower than the electron gas reference).

IV. CONCLUDING REMARKS

The topological analysis of electron localization function (ELF) and the Kohn-Sham local temperature map have been used to characterize the bonding nature of the N_5^+ cation. It is shown that simple analysis of the electron fluctuations between the ELF basins in connection with the examination of the local electronic temperature, yields a picture of bonding which complements previous results based on other methodologies. The pattern of electron fluctuation among the ELF basin populations and the local temperature maps complements and extends our understanding of the currently accepted Eq. (1) to describe the nature of bonding in N_5^+. Indeed, it also agrees to give a picture of bonding which emphasize the strongest correlations observed at N2N3N4 fragment and at the N1N2 and N5N4 regions in this example of non-classical chemical bond.

ACKNOWLEDMENTS

REFERENCES

1R. Ponec, J. Roithová, X. Gironés, and K. Jug, J. Mol. Struc. (Theochem) 545, 255 (2001).   [Links]

2K. O. Christe, W. W. Wilson, J. A. Sheehy, and J. A. Boatz, Angew. Chem. Int. Ed. Engl. 38, 2004 (1999).   [Links]

3(a) R. Ponec, and R. C. Bochicchio, Int. J. Quatum Chem. 54, 99 (1995);   [Links] (b) R. Bochicchio, R. Ponec, A. Torre, and L. Lain, Theor. Chem. Acc. 105, 292 (2001);   [Links] (c) R. Ponec, and R. C. Bochicchio, Int. J. Quantum. Chem. 72, 127 (1999);   [Links] (d) R. C. Bochicchio, R. Ponec, and F. Uhlik, Inorg. Chem. 36, 5363 (1997);   [Links] (e) R. Ponec, K. Jug, Int. J. Quantum Chem. 60, 75 (1996).   [Links]

4(a) R. Ponec, J. Comp. Chem. 20, 760 (1999);   [Links] (b) R. Ponec, and A. J. Duben, J. Comp. Chem. 20, 760 (1999).   [Links]

5T. M. Klapotke, Angew. Chem. Int. Ed. Engl. 38, 2536 (1999).   [Links]

6M. T. Nguyen, T. K. Ha, Chem. Phys. Lett. 135, 317 (2000).   [Links]

7(a) A. Savin, R. Nesper, S. Wengert, and T. F. Fäsler, Ang. Chem. Int. Ed. 36, 1808 (1997);   [Links] (b) D. Max, and A. Savin, Angew. Chem. Int. Ed. 36, 2077 (1997);   [Links] (c) A. Savin, A. D. Becke, J. Flad, R. Nesper, H. Preuss, and H. von Schnering, Angew. Chem. Int. Ed. 30, 409 (1991).   [Links]

8For instance see: (a) J. Melin, and P. Fuentealba, Int. J. Quantum Chem. 92, 381, (2003);   [Links] (b) J. Lundell, S. Berski, and Z. Latajka, Chem. Phys. Letters 371, 295 (2003);   [Links] (c) H. G. von Schnering, J-H. Chang, K. Peters, E.M. Peters, F. R. Wagner, Y. Grin, and G. Thiele, Z. An. Allg. Chem. 629, 516 (2003);   [Links] (d) D. J. Grimwood, I. Bytheway, and D. Jayatilaka, J. Comp. Chem. 24, 470 (2003);   [Links](e) E. Chamorro, P. Fuentealba, and A. Savin, J. Comp. Chem. 24, 496 (2003);   [Links] (f) E. Chamorro, J. Chem. Phys. In Press (2003).   [Links]

9(a) K. Ghosh, M. Berkowitz, and R. G. Parr, Proc. Natl. Acad. Sci. USA. 81, 8028 (1984);   [Links] (b) A. Nagy, and R.G. Parr, Proc. Ind. Acad. Sci. 106, 217 (1994);   [Links] (c) A. Nagy, Reviews of Modern Quantum Chemistry 1, 413 (2002).   [Links]

10P. W. Ayers, R. G. Parr, and A. Nagy, Int. J. Quantum. Chem. 90, 309 (2002).   [Links]

11R. F. Bader, Atoms in Molecules: A Quantum Theory (Oxford University Press, Oxford, 1994).   [Links]

12A. D. Becke, and K. E. Edgencombe, J. Chem. Phys. 92, 5397 (1990).   [Links]

13a) B. Silvi, and A. Savin, Nature, 371, 683 (1994);   [Links] b) A. Savin, B. Silvi, and F. Colonna, Can. J. Chem. 74, 1088 (1996);   [Links] c) S. Noury, F. Colonna, and A. Savin, J. Mol. Struct. 450, 59 (1997).   [Links]

14R. F. W. Bader, Localization and delocalization in quantum chemistry, Edited by O. Chalvet, et. al. (Reidel, Dordrecht, 1976), Vol 1.   [Links]

15For details concerning several applications both in the AIM and ELF schemes see for instance: [Links](a) X. Fradera, J. Poater S. Simon, M. Duran, and M. Sola, Theor. Chem. Acc. 108, 214 (2002);   [Links] (b) J. Poater M. Sola, M. Duran, and X. Fradera, Theor. Chem. Acc. 107, 362 (2002);   [Links] (c) X. Fradera, and M. Sola J. Comp. Chem. 23, 1347 (2002);   [Links] (d) D. B. Chesnut, L. Bartolotti, L. J. Chem. Phys. 257, 175 (2000) ;   [Links] (e) I. Fourré, B. Silvi, P. Chaquin, and A. Sevin, J. Comp. Chem. 20, 897 (1999);   [Links] (f) X. Fradera, M. A. Austen, and R. F. W. Bader, J. Phys. Chem. A. 103, 304 (1999);   [Links] (g) R. Llusar, A. Beltrán, J. Andrés, S. Noury, and B. Silvi, J. Comp. Chem. 20, 1517 (1999);   [Links]

16P. K. Chattaraj, E. Chamorro, and P. Fuentealba, Chem. Phys. Lett. 314, 114 (1999).   [Links]

17H. L. Schmider, and A. D. Becke, J. Mol. Struc. (Theochem) 527, 51 (2000).   [Links]

18(a) V. Tsirelson, A. Stash A Acta Crystallogr. B. 58, 780 (2002);   [Links] (b) H. L Schmider, and A. D. Becke, J. Chem. Phys. 116, 3184 (2002).   [Links]

19Gaussian 98, Revision A.9, M. J. Frisch, G. W. Trucks, H. B. Schlegel, et al. (Gaussian, Inc., Pittsburgh Pennsylvania, 1998).   [Links]

20S. Noury, X. Krokidis, F. Fuster, and B. Silvi, TopMoD package, Universite Pierre et Marie Curie, 1997.   [Links]

21S. Noury, X. Krokidis, F. Fuster, and B. Silvi, B. Comp. Chem.(Oxford) 23, 597 (1999).   [Links]

22(a) B. Hibbard, J. Kellum, and B. Paul, Vis5d 5.1, Visualization Project. University of Winconsin-Madison Space Science and Engineering Center (SSEC);   [Links] (b) B. Hibbard, and D. Santek, Proc. IEEE, 129, 28 (1990).   [Links]